nature geoscience

ARTICLES

PUBLISHED ONLINE: 26 JANUARY 2015 | DOI: 10.1038/NGEO2346

The remote impacts of climate feedbacks on regional climate predictability

Gerard H. Roe[1*], Nicole Feldl[2], Kyle C. Armour[3], Yen-Ting Hwang[4] and Dargan M. W. Frierson[5]

Uncertainty in the spatial pattern of climate change is dominated by divergent predictions among climate models. Model differences are closely linked to their representation of climate feedbacks, that is, the additional radiative fluxes that are caused by changes in clouds, water vapour, surface albedo, and other factors, in response to an external climate forcing. Progress in constraining this uncertainty is therefore predicated on understanding how patterns of individual climate feedbacks aggregate into a regional and global climate response. Here we present a simple, moist energy balance model that combines regional feedbacks and the diffusion of both latent and sensible heat. Our model emulates the relationship between regional feedbacks and temperature response in more comprehensive climate models; the model can therefore be used to understand how uncertainty in feedback patterns drives uncertainty in the patterns of temperature response. We find that whereas uncertainty in tropical feedbacks induces a global response, the impact of uncertainty in polar feedbacks remains predominantly regionally confined.

A central concept in climate science is that the response to a perturbation can be partitioned into individual climate feedbacks. Early studies borrowed the formal language of feedback analysis from control-systems theory, and combined estimates of all major atmospheric feedbacks to predict the global climate sensitivity to radiative forcing[1–3]. Such studies illustrate a central purpose of feedback analysis: it is a powerful method for combining the effects of very different physical processes. In turn this facilitates an important uncertainty analysis: how does uncertainty in the strength of different feedbacks translate into uncertainty in the system response?

An extension of this global-scale work is to characterize regional-feedback patterns, to provide insight into the relative importance of different processes for regional responses. For example, how do subtropical cloud feedbacks affect polar amplification? One widely shared goal is to identify which feedbacks contribute most uncertainty to the temperature response, thereby offering a path to reducing uncertainty in future-climate projections from comprehensive general circulation models (GCMs). Indeed it is hard to imagine how projections can be improved without better constraints on regional feedbacks.

Analyses show broad spreads of feedback patterns among GCMs. For the zonal-mean net feedback (measured in $\mathrm{W\,m^{-2}\,K^{-1}}$, see equation (1)), the spread among 12 models from the third Coupled Model Intercomparison Project[4] (CMIP3) exceeds the multi-model mean at nearly all latitudes, with the spread in shortwave cloud feedback the largest contribution[5]. Several other studies also conclude low-level cloud changes constitute the greatest source of variation among GCMs (refs 6,7).

What to make of this spread in feedback patterns and how to relate it to the range of temperature responses? At any location subject to a climate forcing, the energy budget equilibrates via climate feedbacks modifying the top-of-atmosphere (TOA) radiative fluxes and changes in horizontal energy transport (atmospheric and oceanic). In physical terms, a positive-feedback region is less efficient in radiatively adjusting than a negative-feedback region. Therefore, all else being equal, the system exports energy from positive- to negative-feedback regions. This was demonstrated in detail for an aquaplanet GCM (ref. 8) and within the CMIP3 and CMIP5 ensembles[5,9]. However, these studies just diagnosed patterns of radiative fluxes and transport, and do not explain the pattern of the response.

A path forward is suggested by a study that sought to understand energy-transport changes among the CMIP3 ensemble[10]. After accounting for differences in the surface and TOA fluxes due to clouds and surface albedo, they show the inter-model spread in energy-transport changes is predicted well by an energy balance model diffusing low-level moist static energy (MSE), a formulation accounting for both sensible- and latent-heat changes[11]. The result is important: despite all the structural and parametric differences among highly complex GCMs, a simple principle governs their underlying behaviour. A similar model, diffusing a linearized version of MSE, emulates the response of aquaplanet GCMs forced with patterns of ocean heat uptake[12].

Collectively these studies indicate that the pattern of the temperature response can be predicted from the pattern of change in the TOA fluxes and the down-gradient transport of MSE anomalies. We employ an extension of this moist static energy balance model (MEBM) to address two issues. First, we show how the pattern of feedbacks controls the pattern of temperature response, finding that the MEBM successfully emulates an aquaplanet GCM, both with and without ice-albedo feedback. Second, we demonstrate how uncertainty in the pattern of feedbacks drives uncertainty in the pattern of the response.

[1]Department of Earth and Space Sciences, University of Washington, Seattle, Washington 98103, USA. [2]Environmental Science and Engineering, California Institute of Technology, Pasadena, California 91125, USA. [3]Department of Earth, Atmospheric, and Planetary Sciences, Massachusetts Institute of Technology, Cambridge, Massachusetts 02139, USA. [4]Department of Atmospheric Sciences, National Taiwan University, Taipei 10673, Taiwan. [5]Department of Atmospheric Sciences, University of Washington, Seattle, Washington 98103, USA. *e-mail: gerard@ess.washington.edu

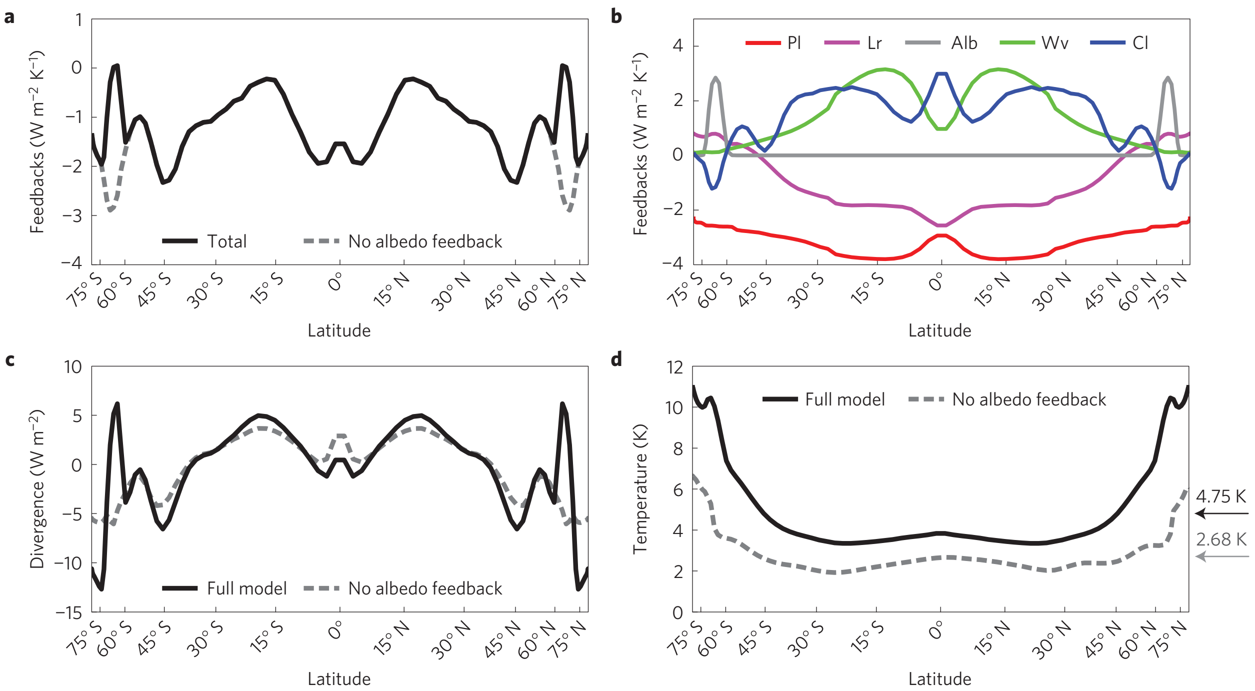

Figure 1 | The relationship between feedback patterns and climate response in aquaplanet GCM simulations. a, Total feedback (solid), surface-albedo feedback suppressed (dashed). **b**, Individual, locally defined Planck response (Pl), lapse-rate (Lr), surface-albedo (Alb), water-vapour (Wv) and cloud (Cl) feedbacks, modified from ref. 17 to include a logarithmic dependence of water-vapour feedback (ref. 41). **c**, Changes in the convergence/divergence of heat transport after CO_2 doubling. **d**, Temperature response for a CO_2 doubling, with global mean indicated with arrows. Latitude axes are presented in equal-area increments in all figures.

The local and nonlocal impacts of climate feedbacks

Let $T'(x)$ be the annual-mean, near-surface air temperature response to a forcing, $R_f(x)$, as a function of the sine latitude, x. In equilibrium this forcing is balanced by changes in atmospheric and oceanic heat-flux divergence, $\nabla \cdot \mathbf{F}'(x)$, plus the sum of fluxes from radiative feedbacks, $\sum_i c_i(x)T'(x)$—the first-order terms in a Taylor series of the TOA radiative response to warming.

$$-R_f(x) = -\nabla \cdot \mathbf{F}'(x) + \sum_{i=1}^{N} c_i(x)\, T'(x) \qquad (1)$$

Neglecting the second-order and higher terms in the Taylor series is conventional in feedback analysis and is justified, at least for anthropogenic climate-change scenarios, on the basis of detailed analyses of climate models[8,13–16]. The nature of the temperature response and the feedbacks (that is, the coefficients $c_i(x)$) that drive it are most clearly elucidated in GCMs configured for idealized experiments. Figure 1 shows the feedback, transport changes and surface-temperature response to a CO_2 doubling in a mixed-layer aquaplanet version of the Geophysical Fluid Dynamics Laboratory (GFDL) AM2 model, an atmospheric GCM configured here with simple thermodynamic sea ice[8,17]. The $c_i(x)$ values were calculated using the radiative-kernel method[8,14,17] which best approximates the tangent-linear ideal of the Taylor series (equation (1)) and includes Planck, water-vapour, surface-albedo, lapse-rate and cloud feedbacks. We note that feedbacks are defined here relative to the local, rather than the global-mean, temperature[17–20].

The pattern of heat-transport changes (solid line, Fig. 1c) bears a striking similarity to the pattern of net feedback (solid line, Fig. 1a): energy fluxes diverge from the subtropics owing to strongly positive water-vapour and cloud feedbacks (Fig. 1b), and converge into midlatitudes where feedbacks are more negative. Energy fluxes also diverge from positive feedbacks at the ice line, resulting in energy convergence polewards of the ice line. This convergence is the largest contribution to the temperature response at high latitudes, although other feedbacks also matter, notably a positive lapse-rate feedback due to near-surface-temperature inversions (Fig. 1b)[8,17,21]. The similarity between $\nabla \cdot \mathbf{F}'(x)$ and $\sum_i c_i(x)$, both diagnosed from the GCM, also demonstrates the ability of the linear feedback framework (that is, equation (1)) to describe the changes in the TOA energy budget in the GCM.

Another experiment is performed here, suppressing the surface-albedo feedback by fixing the ice line[22] (dashed lines, Fig. 1). The results are remarkable. Removing the surface-albedo feedback results in only a small change in the overall feedback pattern (Fig. 1a), and the biggest difference in transport changes is the loss of the high-latitude dipole of heat-flux divergence/convergence (Fig. 1c). However, despite these apparently minor differences, the global-mean temperature response is nearly halved (from 4.75 °C to 2.68 °C, Fig. 1d), and there is a marked reduction in polar amplification. Evidently this local feedback drives significant local and nonlocal responses. Although striking, these results conform to the basic principle that systems of strongly positive feedbacks are acutely sensitive to small changes in feedback strength[2,23].

The importance of MSE

The latent heat associated with water-vapour changes is central to the climate response, and can be characterized using the near-surface MSE ($h' \equiv c_p T' + L_v q'$; c_p is specific heat at constant pressure, T' is annual-mean temperature change, L_v is latent heat of vaporization and q' is change in specific humidity). For fixed relative humidity (assumed 80%), q' is governed by the Clausius–Clapeyron relation, and is a sensitive function of T'.

At 30 °C, a warming of $T' = 1$ °C corresponds to $h' \approx 4{,}000$ J kg^{-1}, whereas at −20 °C that same 1 °C warming yields only $h' \approx 1{,}100$ J kg^{-1}. In other words, owing to the climatological pole-to-equator temperature gradient, there is inevitably a strong weighting of h' towards the tropics.

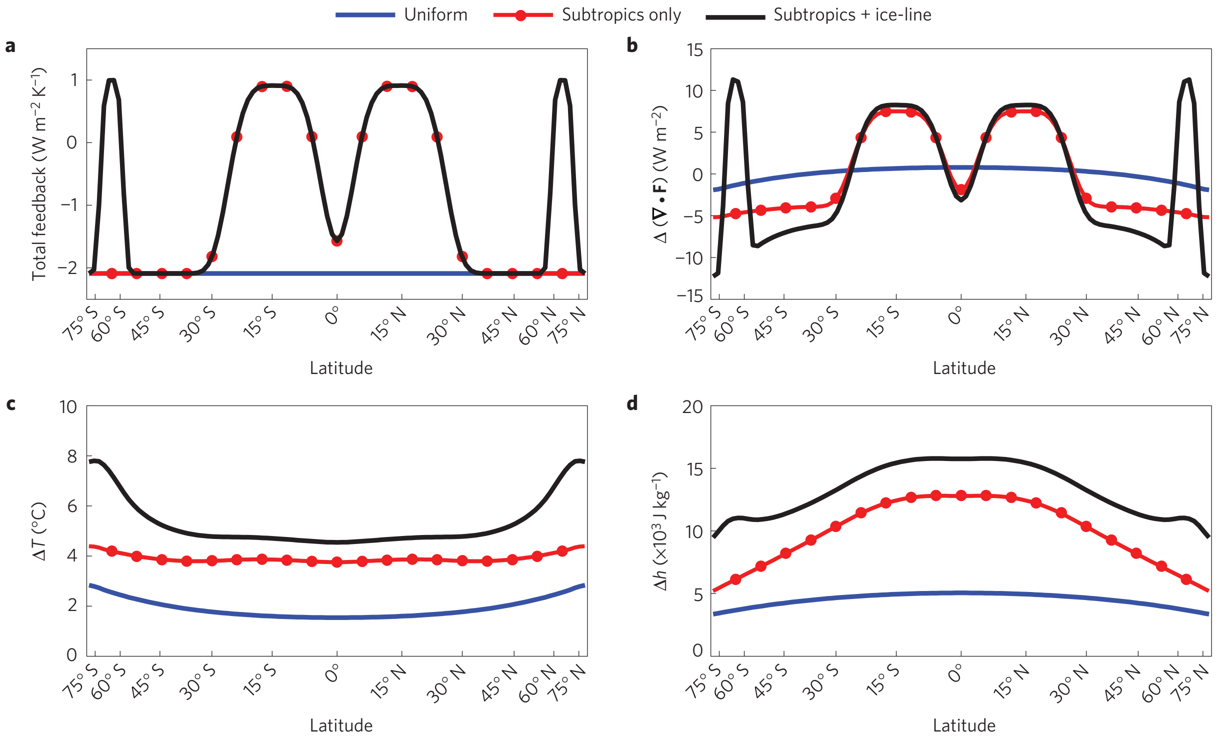

Figure 2 | The climate response in the moist energy balance model for three different, stylized feedback patterns. a, Feedback patterns. **b**, Change in heat-transport convergence/divergence ($\nabla \cdot \mathbf{F}'$). **c**, Change in temperature, T'. **d**, Change in MSE, h'. For the three experiments the global-mean temperature increases are 1.9, 3.9, and 5.3 °C respectively.

A reasonable starting point is to suppose a down-gradient flux of h' anomalies, the simplest formulation for which is Fickian diffusion: $\mathbf{F}' = -D\nabla h'$, where D is a constant[11,24]. Mixing-length theory suggests D is proportional to a length scale times a velocity scale[25]. Both change relatively slowly under climate change[26,27], justifying a diffusivity that remains constant. For zonal-mean fields on a sphere, this yields

$$\nabla \cdot \mathbf{F}' = -D \frac{\mathrm{d}}{\mathrm{d}x}\left(1-x^2\right)\frac{\mathrm{d}h'}{\mathrm{d}x} \qquad (2)$$

Equation (2) is intended to characterize atmospheric heat transport. Changes in oceanic heat uptake evolve slowly, and so can be conceived of as a forcing term on the atmosphere, and subsumed into $R_f(x)$, although it must be established that the pattern of atmospheric feedbacks remains robust[12,20]. Equations (1) and (2) constitute an idealized MEBM that can be solved for the pattern of temperature response, $T'(x)$, as a function of the patterns of $R_f(x)$ and the coefficients $c_i(x)$. To focus on the feedback patterns, we set constant $R_f = 4\,\mathrm{W\,m^{-2}}$ and use $D = 2.6 \times 10^{-4}\,\mathrm{kg\,m^{-2}\,s^{-1}}$ throughout[10]. We note that classic energy balance climate models[28] diffuse only sensible heat (that is, c_pT') and behave very differently from the MEBM; and whereas in ref. 10 the $c_i(x)T'(x)$ terms in equation (1) are diagnosed from CMIP3 CGMs, here only the $c_i(x)$ values are stipulated and $T'(x)$ is calculated self-consistently within the MEBM.

Even for spatially uniform feedbacks, the MEBM exhibits substantial polar amplification (blue lines, Fig. 2): larger h' anomalies in the moist tropics drive a poleward energy flux[11], and the resulting extratropical convergence generates larger T' there (Fig. 2b,c).

We next impose broad zones of positive subtropical feedbacks, similar in form to those in the aquaplanet GCM (Fig. 1a), which approximately double the global-mean temperature response (red line with circle symbols, Fig. 2). Further, where $\sum c_i(x) > 0$ the system is locally unstable, and it must adjust by exporting h' (Fig. 2b): strong subtropical divergence (a cooling tendency) must be matched by extratropical convergence (a warming tendency). These transport changes can be accomplished with relatively small tropical temperature changes because the q' there leads to large changes in h' (Fig. 2c,d). Thus, even when strong local feedbacks in the subtropics favour a large local response, their nonlocal impact maintains a slight degree of polar amplification.

Last, we introduce another, narrow band of positive feedbacks at 65° latitude (black lines, Fig. 2), representative of ice-albedo feedback at an ice line. This local feedback drives a large local divergence of energy, balanced by convergence predominantly polewards of the ice line (Fig. 2b,d). Owing to the low temperatures at these latitudes, q' contributes little to h', and so the convergence produces a large change in T' (~ 8 °C) and strong polar amplification.

The MEBM thus mirrors the aquaplanet GCM: feedback patterns drive both a local response and a change in heat-flux divergence; the strong tropical weighting of h' leads to increased poleward energy fluxes; and at high latitudes a large T' is required to balance flux convergence changes because of the relative lack of moisture there. It is the interplay among these tendencies that sets the response. There are of course some differences; for instance, the polar amplification is less pronounced in the MEBM without ice-line albedo feedback. Our assumption of Fickian diffusion is surely too simplistic to emulate every detail of the temperature response—particularly where eddies are not dominant, such as in the deep tropics—and we have used only stylized feedback patterns. Nevertheless, the basic similarities, together with the ability of the MEBM to account for transport changes among ensembles of fully coupled GCMs (refs 10,29,30), lend confidence it can be used to infer the impact of uncertainty in the magnitude and pattern of climate feedbacks on uncertainty in the magnitude and pattern of the temperature response.

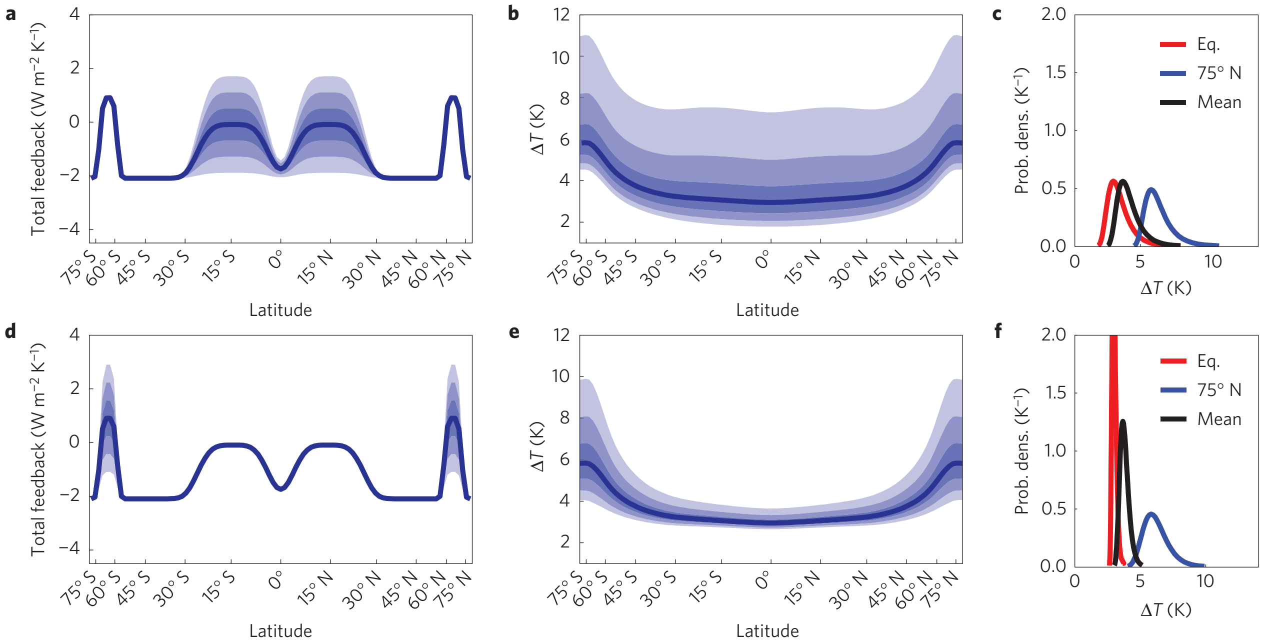

Figure 3 | The impact of uncertainty in feedbacks patterns on uncertainty in temperature-response patterns in the moist energy balance model. **a**–**c**, Subtropical feedback uncertainty (**a**), temperature response (**b**), response PDF at specific latitudes (**c**). **d**–**f**, As for **a**–**c**, but for the ice line feedback uncertainty. Feedback uncertainty has the form: $c(x)=c_0(x)+\sigma_c \exp(-[(x-x_0)/\Delta x]^4)$; $c_0(x)$ is mean feedback pattern; $\sigma_c=0.6$ W m^{-2} K^{-1}; $(x_0,\Delta x)=(\pm 0.25, 0.2)$ for subtropical feedbacks and $(\pm 0.9, 0.05)$ for ice-line feedbacks. In **a**, **b**, **d**, **e** the solid line is the mean value, and the shading represents the 1−, 2−, and $3-\sigma$ ranges.

Feedback uncertainty and regional predictability

We introduce feedback uncertainties into the MEBM, by stipulating localized zones of Gaussian probability density functions (PDFs) in the subtropics and poles. These are hypothetical, but guided by GCM ensembles[5].

Uncertainty in subtropical feedbacks (Fig. 3a) leads to uncertainty in T' that is global and nearly uniform (Fig. 3b). The feedback uncertainty induces large uncertainty in subtropical h', which is exported down gradient to mid- and high latitudes, where it drives uncertainty in T'. Therefore, reducing uncertainty in tropical feedbacks would lead to a globally near-uniform reduction of uncertainty in temperature response. At all latitudes, the PDF is skewed towards higher T' (Fig. 3c) because larger positive feedbacks destabilize the system[23].

In contrast, uncertainty in polar feedbacks (Fig. 3d) leads to uncertainty in T' confined largely to the poles (Fig. 3e): the resulting variations in h' are not large enough to overcome the large-scale, down-gradient transport of h' from the tropics, and therefore distribute much less uncertainty into lower latitudes. The implication is that a reduction of uncertainty in polar feedbacks leads to a predominantly local reduction of uncertainty in temperature response. Note, however, that even small changes in tropical temperatures can impact other important aspects of climate, such as the inter-tropical convergence zone and monsoon circulations, and thus our results do not preclude polar feedbacks exerting an influence on such climate features[31,32].

Uncertainty in temperature response thus depends on both the magnitude and spatial extent of the uncertainty in local feedbacks. The feedback patterns in Fig. 3a,d reflect relatively broad uncertainty within the subtropics (for example, due to changes in clouds) and relatively narrow uncertainty near the poles (for example, due to changes in the sea-ice edge)[5]. This difference in spatial extent affects the uncertainty in global-mean temperature response, with subtropical feedback uncertainty having a stronger global influence than the high-latitude uncertainty (black lines, Fig. 3c,f). However, for feedback uncertainty of equivalent magnitude and area, it is the high latitudes that matter more for the global mean (Supplementary Fig. 1); feedback uncertainty projects most strongly onto the global-mean temperature response when it coincides with a region of large temperature change and of more positive local feedbacks—conditions that apply at high latitudes (Fig. 3 and see Supplementary Information).

Internal (that is, unforced) climate variability is an important uncertainty in regional climate projections on decadal timescales[33]. On longer timescales two factors dominate uncertainty: the anthropogenic-forcing scenario and structural differences among GCMs (ref. 34). Several lines of research demonstrate that, on such timescales, adjustments to Earth's energy budget occur via MSE fluxes driven by patterns of climate feedbacks. The simplest implementation—the MEBM—accords with detailed feedback calculations within a GCM: anomalous energy fluxes diverge away from regions of more positive feedbacks, and converge towards regions of more negative feedbacks. Although it will be important to establish the limitations of the MEBM and the linear feedback framework for larger climate changes[35,36], as well as the approximation that feedbacks can be described locally (that is, independently of the pattern of warming itself), it offers a single, consistent explanation for several fundamental aspects of climate change pervasive among GCM simulations: a general increase in poleward energy fluxes with global warming[10,37]; strong polar amplification, but with large inter-model spread[38]; and uncertainty in broad tropical feedbacks being the largest source of uncertainty in the global temperature response[7,39]. Other recent studies imply the principle also extends to transient climate change, to more complete GCMs and, tentatively, to zonally asymmetric feedbacks[10,12,23,40]. Collectively these studies can be taken as implying that circulation changes may be of secondary importance in redistributing energy under climate change. The underlying principle does not depend on which climate processes are acting, only on the overall pattern of total climate feedback. However, by disaggregating the climate response into its component feedbacks, the relative importance of particular processes for the local and nonlocal response can be deciphered. Although the true patterns of the various climate feedbacks remain elusive, understanding these connections is a prerequisite for constraining uncertainty at regional scales, where the environmental and societal impacts of global climate change are predominantly experienced.

Received 8 August 2014; accepted 16 December 2014; published online 26 January 2015

References

1. Charney, J. G. *et al. Carbon Dioxide and Climate: A Scientific Assessment* 22 (National Academy of Sciences, 1979).
2. Hansen, J. E. *et al.* in *Climate Processes and Climate Sensitivity* (eds Hansen, J. E. & Takahashi, T.) 130–163 (American Geophysical Union, 1984).
3. Schlesinger, M. E. in *The Potential Climatic Effects of Increasing Carbon Dioxide* (eds MacCracken, M. & Luther, F.) 81–147 (US Dept. of Energy, 1985).
4. Meehl, G. A. *et al.* The WCRP CMIP3 multi-model dataset: A new era in climate change research. *Bull. Am. Meteorol. Soc.* **88,** 1383–1394 (2007).
5. Zelinka, M. A. & Hartmann, D. L. A diagnostic study of climate feedback processes in atmospheric general circulation models. *J. Clim.* **25,** 608–624 (2012).
6. Soden, B. J. & Vecchi, G. A. The vertical distribution of cloud feedback in coupled ocean–atmosphere models. *Geophys. Res. Lett.* **38,** L12704 (2011).
7. Bony, S. & Dufresne, J. L. Marine boundary layer clouds at the heart of cloud feedback uncertainties in climate models. *Geophys. Res. Lett.* **32,** L20806 (2005).
8. Feldl, N. & Roe, G. H. The nonlinear and nonlocal nature of climate feedbacks. *J. Clim.* **26,** 8289–8304 (2013).
9. Huang, Y. & Zhang, M. The implication of radiative forcing and feedback for meridional energy transport. *Geophys. Res. Lett.* **41,** 1665–1672 (2014).
10. Hwang, Y-T. & Frierson, D. M. W. Increasing atmospheric poleward energy transport with global warming. *Geophys. Res. Lett.* **37,** L24807 (2010).
11. Flannery, B. P. Energy balance models incorporating transport of thermal and latent energy. *J. Atmos. Sci.* **41,** 414–421 (1983).
12. Rose, B. E. J. *et al.* The dependence of transient climate sensitivity and radiative feedbacks on the spatial pattern of ocean heat uptake. *Geophys. Res. Lett.* **41,** 1071–1078 (2014).
13. Bony, S. *et al.* How well do we understand and evaluate climate change feedback processes? *J. Clim.* **19,** 3445–3482 (2006).
14. Soden, B. J. & Held, I. M. An assessment of climate feedbacks in coupled ocean atmosphere models. *J. Clim.* **19,** 3354–3360 (2006).
15. Roe, G. H. Feedbacks, time scales, and seeing red. *Annu. Rev. Earth Planet. Sci.* **37,** 93–115 (2009).
16. Roe, G. H. & Armour, K. C. How sensitive is climate sensitivity? *Geophys. Res. Lett.* **38,** L14708 (2011).
17. Feldl, N. & Roe, G. H. Four perspectives on climate feedbacks. *Geophys. Res. Lett.* **40,** 4007–4011 (2013).
18. Boer, G. J. & Yu, B. Climate sensitivity and climate state. *Clim. Dynam.* **21,** 167–176 (2003).
19. Crook, J. A., Forster, P. M. & Stuber, N. Spatial patterns of modeled climate feedback and contributions to temperature response and polar amplification. *J. Clim.* **24,** 3575–3592 (2011).
20. Armour, K. C., Bitz, C. M. & Roe, G. H. Time-varying climate sensitivity from regional feedbacks. *J. Clim.* **26,** 4518–4534 (2013).
21. Mauritsen, T. *et al.* Climate feedback efficiency and synergy. *Clim. Dynam.* **41,** 2539–2554 (2013).
22. Graversen, R. G. & Wang, M. Polar amplification in a coupled climate model with locked albedo. *Clim. Dynam.* **33,** 629–643 (2009).
23. Roe, G. H. & Baker, M. B. Why is climate sensitivity so unpredictable? *Science* **318,** 629–632 (2007).
24. Frierson, D. M. W., Held, I. M. & Zurita-Gotor, P. A gray-radiation aquaplanet moist GCM. part II: Energy transports in altered climates. *J. Atmos. Sci.* **64,** 1680–1693 (2007).
25. Vallis, G. K. *Atmospheric and Oceanic Fluid Dynamics* (Cambridge Univ. Press, 2006).
26. Kidston, J., Dean, S. M., Renwick, J. A. & Vallis, G. K. A robust increase in the eddy length scale in the simulation of future climates. *Geophys. Res. Lett.* **37,** L03806 (2010).
27. O'Gorman, P. A. Understanding the varied response of the extratropical storm tracks to climate change. *Proc. Natl Acad. Sci. USA* **107,** 19176–19180 (2010).
28. North, G. R., Cahalan, R. F. & Coakley, J. K. Jr Energy balance climate models. *Rev. Geophys.* **19,** 91–121 (1981).
29. Hwang, Y-T., Frierson, D. M. W. & Kay, J. E. Coupling between Arctic feedbacks and changes in poleward energy transport. *Geophys. Res. Lett.* **38,** L17704 (2011).
30. Frierson, D. M. W. & Hwang, Y-T. Extratropical influence on ITCZ shifts in slab ocean simulations of global warming. *J. Clim.* **25,** 720–733 (2012).
31. Chiang, J. C. H. & Bitz, C. M. Influence of high latitude ice cover on the marine Intertropical Convergence Zone. *Clim. Dynam.* **25,** 477–496 (2005).
32. Pausata, F., Battisti, D. S., Nisancioglu, K. N. & Bitz, C. M. Chinese stalagmites: Proxies for the Indian monsoon response to an archetypal Heinrich event. *Nature Geosci.* **4,** 474–480 (2011).
33. Deser, C., Phillips, A. S., Bourdette, V. & Teng, H. Uncertainty in climate change projections: The role of internal variability. *Clim. Dynam.* **38,** 527–546 (2012).
34. Hawkins, E. & Sutton, R. The potential to narrow uncertainty in regional climate predictions. *Bull. Am. Meteorol. Soc.* **90,** 1095–1107 (2009).
35. Caballero, R. & Hanley, J. Midlatitude eddies, storm-track diffusivity and poleward moisture transport in warm climates. *J. Atmos. Sci.* **69,** 3237–3250 (2012).
36. Caballero, R. & Huber, M. State-dependent climate sensitivity in past warm climates and its implications for future climate projections. *Proc. Natl Acad. Sci. USA* **110,** 14162–14167 (2013).
37. Wu, Y. *et al.* Changes in storm tracks and energy transports in a warmer climate simulated by the GFDL CM2.1 model. *Clim. Dynam.* **37,** 53–72 (2011).
38. Holland, M. M. & Bitz, C. M. Polar amplification of climate change in the coupled model intercomparison project. *Clim. Dynam.* **21,** 221–232 (2003).
39. Webb, M. J., Lambert, F. H. & Gregory, J. M. Origins of differences in climate sensitivity, forcing and feedback in climate models. *Clim. Dynam.* **40,** 677–707 (2013).
40. Feldl, N., Frierson, D. M. W. & Roe, G. H. The influence of regional feedbacks on circulation sensitivity. *Geophys. Res. Lett.* **41,** 2212–2220 (2014).
41. Held, I. M. & Soden, B. J. Water vapor feedback and global warming. *Annu. Rev. Energy Environ.* **25,** 441–475 (2000).

Acknowledgements

The authors are grateful for enlightening feedback from M. Baker, A. Donohoe and P. Molnar.

Author contributions

G.H.R. performed the MEBM analyses and N.F. performed the AM2 integrations. All authors contributed to the interpretation of the results and to writing the manuscript.

Additional information

Supplementary information is available in the online version of the paper. Reprints and permissions information is available online at www.nature.com/reprints. Correspondence and requests for materials should be addressed to G.H.R.

Competing financial interests

The authors declare no competing financial interests.